Characterization of Mo−P−Alumina Sol−Gel Catalysts by Solid-State ^{31}P and ^{27}Al Magic-Angle Spinning Nuclear Magnetic Resonance and Two-Dimensional ^{27}Al Multiple-Quantum Magic-Angle Spinning Nuclear Magnetic Resonance

R. Iwamoto,[†,‡] C. Fernandez,[§] J. P. Amoureux,[§] and J. Grimblot*[,†]

Laboratoire de Catalyse Hétérogène et Homogène, URA CNRS 402, Université des Sciences et Technologies de Lille, 59655 Villeneuve d'Ascq Cédex, France, Petroleum Refining Technology Center, Idemitsu Kosan Co. Ltd., 1280 Kami-izumi, Sodegaura, Chiba, 299-02, Japan, and Laboratoire de Dynamique et Structure des Matériaux Moléculaires, URA CNRS 801, Université des Sciences et Technologies de Lille, 59655 Villeneuve d'Ascq Cédex, France

Received: November 21, 1997; In Final Form: March 12, 1998

Conventional solid-state ^{27}Al and ^{31}P magic-angle spinning nuclear magnetic resonance (MAS NMR) and an advanced two-dimensional ^{27}Al multiple-quantum MAS NMR (2D ^{27}Al MQMAS NMR) have been applied to characterize $MoO_3-P_2O_5-Al_2O_3$ hydrotreating catalysts. These catalysts were prepared by a sol−gel method with high Mo loadings (with Mo expected amounts of ∼20 and ∼30 wt %) and a wide range of P content (from 0 to 13 wt % of P). The chemical environments of Al and P strongly depend on the nature of the P precursor used in the sample preparation (H_3PO_4 or P_2O_5) and on the amount of P and Mo. From the ^{27}Al MAS NMR measurements on dried P-containing samples, formation of octahedral aluminum (Al_{octa}) and of $AlPO_4$ ($Al_{tetra}-O-P$ surface species) in small amounts was observed. After calcination at 500 °C, the formation of tetrahedral aluminum (Al_{tetra}) and pentacoordinated aluminum (Al_{penta}) was also observed. The presence of molybdenum favored the interaction of phosphorus with the alumina framework, leading to significant amounts of $Al_{tetra}-O-P$. At higher P and Mo loadings, $Al_2(MoO_4)_3$ was also detected in the calcined sample. ^{31}P MAS NMR measurements revealed the formation of monomeric or polymeric P oxocompounds after drying and polymeric P oxocompounds or $AlPO_4$ after calcination, respectively. The use of P_2O_5 as a P precursor gave rise to the formation of polymerized P oxocompounds rather than of $AlPO_4$ after calcination in the absence of Mo. 2D ^{27}Al MQMAS NMR gave an improved resolution compared with conventional ^{27}Al MAS NMR. In dried samples, pure alumina and MoO_3−alumina showed a single distorted Al_{octa} site while P-containing catalysts showed additional octahedral and tetrahedral aluminum sites interacting with phosphorus ($Al_{octa}-O-P$ and $Al_{tetra}-O-P$, respectively). After calcination, mainly Al_{octa} and Al_{tetra} sites with a small amount of Al_{penta} sites were observed in pure alumina. The presence of Mo introduced a large distortion in the alumina framework, since the amount of Al_{penta} significantly increased in the presence of Mo. $Al_{tetra}-O-P$ sites were also detected in P-containing alumina catalysts, but the $Al_{octa}-O-P$ sites disappeared after calcination.

Introduction

The active phase of hydrotreating catalysts generally consists of molybdenum sulfide (MoS_2) deposited on γ-alumina. The molybdenum precursor is usually introduced on the alumina support by a conventional wet impregnation method. However, only 10−12 wt % Mo can be dispersed by this procedure. In previous studies, the present authors proposed a new catalyst preparation method based on a sol−gel synthesis.[1,2] In this method, well-dispersed Mo oxospecies on a high surface area alumina support is obtained by hydrolysis of an aluminum alkoxide in the presence of Mo precursor.[1,2] This advanced method can produce powders containing up to ∼30 wt % of well-dispersed Mo with a specific surface area higher than 400 $m^2\ g^{-1}$. To improve the sol−gel hydrotreating catalysts, it appeared interesting to investigate the effects of phosphorus addition during the gel synthesis, since P has already been reported as an excellent promotor for several hydrotreating reactions such as HDS (hydrodesulfurization), HDN (hydrodenitrogenation), and HYD (hydrogenation), as well as the classical promotors such as Co and Ni.[3−6] With phosphorus addition, it was found that the specific surface area of sol−gel catalysts decreases with increasing P loading but may remain relatively high in some cases.[2] XRD (X-ray diffraction) measurements also revealed that large amounts of molybdenum and phosphorus in the catalyst formulation provoke aggregation of bulk MoO_3.[2]

Solid-state NMR is widely known as one of the most useful techniques for characterizing catalysts that may be rather amorphous and with a large number of structural defects. In particular, a considerable number of studies have been carried out to investigate the chemical states and environments of P and Al in $MoO_3-P_2O_5-Al_2O_3$ (Mo−P−alumina) based hydrotreating catalysts.[7−14] The state of P on alumina strongly depends on its amount. At low P content, P is supported as well-

* To whom correspondence should be addressed. Telephone: 33-(0)3 20 43 45 38. Fax: 33-(0)3 20 43 65 61. E-mail: jean.grimblot@univ-lille1.fr.

[†] Laboratoire de Catalyse Hétérogène et Homogène, Université des Sciences et Technologies de Lille.

[‡] Petroleum Refining Technology Center.

[§] Laboratoire de Dynamique et Structure des Matériaux Moléculaires, Université des Sciences et Technologies de Lille.

S1089-5647(98)00291-0 CCC: $15.00
Published on Web 05/12/1998

dispersed mono- or diphosphates. With increasing the P loading, polymeric P oxocompounds and $AlPO_4$ with different degrees of hydration are also formed. In the presence of both Mo and P, the formation of a Mo−P heteropolyanion like $P_2Mo_5O_{23}^{6-}$ is observed while it gradually decomposes to PO_4^{3-} and MoO_4^{2-} after impregnation on the alumina support.[9,12] At higher P loading, the $Al_2(MoO_4)_3$ phase or $[Al(OH)_n(H_2O)_{6-n}]_n(MoO_4)$ (with $n = 1$ or 2) species are also detected by ^{27}Al magic-angle spinning nuclear magnetic resonance (MAS NMR) after calcination. Aluminum cations are mainly located in octahedral or tetrahedral coordination sites, while pentacoordinated Al sites are also found in some cases.[15,16]

Recently, Kraus and co-workers[17,18] applied new advanced NMR techniques such as $^{27}Al-^{31}P$ rotational-echo double resonance (REDOR), transfer of populations in double resonance (TRAPDOR), multiple-quantum magic-angle spinning (MQMAS), and off-resonance quadrupolar nutation to characterize these catalysts more precisely. These techniques revealed that most of P is in close contact with alumina with predominant formation of $AlPO_4$,which possesses a monolayer structure with a slightly higher degree of ordering than the amorphous ones. Formation of stacked phosphate layers and bulk phosphates is excluded.

The objectives of the present study are to give a detailed identification of the states and environments of Al and P on the Mo−P−alumina based sol−gel catalysts by using solid-state ^{27}Al or ^{31}P MAS NMR and two-dimensional ^{27}Al MQMAS NMR. Theories and principles of the MQMAS NMR technique are not discussed here, since they were already given elsewhere.[19−21]

Experimental Section

Catalyst Preparation. The details of the preparation procedure of Mo−P−alumina based sol−gel catalysts, the list of catalysts, and their main characteristics (atomic composition, specific surface area) were already described.[2] Two series of catalysts with expected Mo loadings of 20 and 30 wt % on the Mo element basis (actually, their contents were ∼17 and ∼26 wt % Mo, respectively) and a wide range of P content (from 1 to 13 wt % P) were prepared from hydrolysis of aluminum *sec*-butylate (ASB) in the presence of ammonium heptamolybdate and a phosphorus precursor. For comparison purposes, reference catalysts such as pure alumina, P−alumina, and Mo−alumina were also prepared. Orthophosphoric acid (H_3PO_4) and phosphorus pentoxide (P_2O_5) were selected as P precursors to investigate their effect. The Mo−P (MP) catalysts obtained at each stage are noted as MPD(*X*, *Y*)H or MPC(*X*, *Y*)P where "MPD" or "MPC" means a dried "D" or a calcined "C" sample with *X* wt % of Mo and *Y* wt % of P, respectively (contents expected from the preparation procedure). H or P refers to the nature of P precursor such as H_3PO_4 or P_2O_5, respectively.

NMR Measurements. Conventional solid-state ^{27}Al MAS NMR spectra were obtained from a Bruker ASX400 spectrometer operating at a resonance frequency of 104.26 MHz with a recycling time of 3 s and a short pulse time of 1 μs. The spinning frequency was ∼15 kHz, and $Al(H_2O)_6^{3+}$ was taken as a reference. ^{31}P MAS NMR spectra were obtained from a Bruker ASX100 spectrometer operating at a resonance frequency of 40.53 MHz with a recycling time of 40 s and a pulse time of 2 μs. The spinning frequency was ∼7 kHz, and H_3PO_4 was taken as a reference.

Liquid-state ^{31}P NMR spectra were also recorded to identify the nature of the P species present in the preparation solution. They were obtained on a Bruker ASX300 spectrometer operating at a resonance frequency of 121.50 MHz with a recycling time of 1 s and a pulse time of 2 μs. H_3PO_4 was taken as a reference. The H_3PO_4 and P_2O_5 precursors were dissolved in 2-butanol with a concentration corresponding to the preparation of MPC-(0, 11)H or MPC(0, 12)P catalyst (Mo and ASB were not introduced in these measurements).

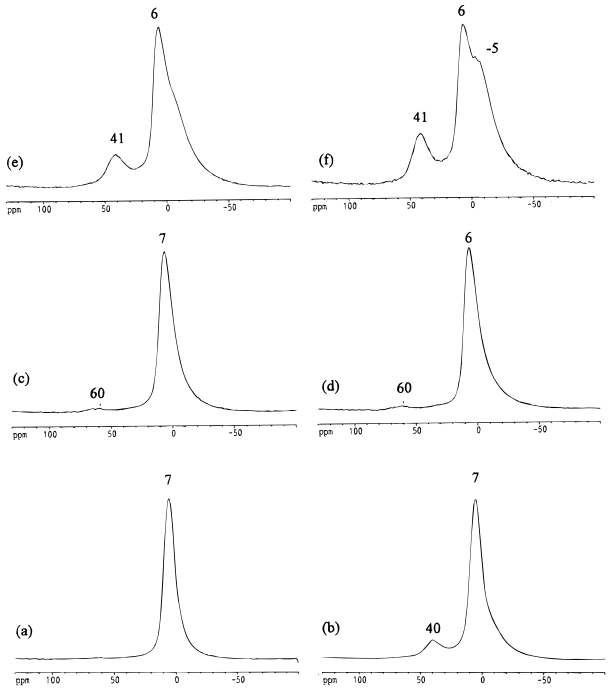

Figure 1. ^{27}Al MAS NMR spectra of Mo−P−alumina based sol−gel catalysts obtained after the drying stage at 100 °C: (a) MPD(0, 0); (b) MPD(0, 11)H; (c) MPD(20, 0); (d) MPD(30, 0); (e) MPD(20, 11)H; (f) MPD(30, 11)H. The P-containing catalysts were prepared with H_3PO_4 as a P precursor.

The details of the experimental procedures for the 2D ^{27}Al MQMAS NMR measurements were already described.[19−21] The spectra were obtained with the Z filtering method[22] from a Bruker ASX400 spectrometer working at 104.3 MHz. Samples were spun at ∼13 kHz. The recycling time was 1 s. The pulse lengths and rf fields were 2 and 0.8 μs with 250 kHz and 8.3 μs with 10 kHz for the two first hard pulses and the selective 90° pulse, respectively. Decoupling for protons was applied systematically. The t_1 increment was chosen to be equal to the inverse of the rotor period in order to minimize the number of experiments needed (128) in the multiple-quantum dimension. For the 3Q MAS measurements, six-phase cycling was combined with an overhall classical cyclops four-phase cycle in order to minimize phase and amplitude mis-settings of the receiver. The minimum number of accumulations to be realized was thus 24 for each t_1 step. In this study, only the trends in the variations of the chemical shifts will be discussed. No quantitative data for quadrupolar interaction will be reported, since the quantitative analysis of 2D ^{27}Al MQMAS NMR may be somehow delicate owing to spectral broadening and overlapping.

Results and Discussion

^{27}Al MAS NMR. *(a) Samples Obtained with H_3PO_4 as a P Precursor*. Figure 1 shows the ^{27}Al MAS NMR spectra of the dried sol−gel catalysts obtained with H_3PO_4 as a P precursor. Table 1 also shows the list of chemical shifts and their assignments obtained in reference compounds. Within the measurement conditions, spinning sidebands cannot be theoretically observed in this region. Although it is somehow difficult

TABLE 1: List of Chemical Shifts and Their Assignments of ^{27}Al MAS NMR for Mo−P−Alumina Sol−Gel Catalysts

δ ppm	Al species	ref compounds or environments	ref
∼−15	Al_{octa}−O−Mo	$Al_2(MoO_4)_3$	11
−5 to −30	Al_{octa}−O−P	$Al(H_2O)_n(OP)_{6-n}$	23
0 to 10[a]	Al_{octa}	γ-alumina	15
		$Al(H_2O)_n(OR)_{6-n}$	
10	Al_{octa}−O−R	unreacted alkoxide	26
13		$[Al(OH)_n(H_2O)_{6-n}]_n(MoO_4)$ ($n = 1, 2$)	10
14	Al_{penta}−O−P	$Al(H_2O)_n(OP)_{5-n}$	28
∼30	Al_{penta}	distorted γ-alumina	16
∼40	Al_{tetra}−O−P	$AlPO_4$	8
53 to 75[a]	Al_{tetra}	γ-alumina	15

[a] The chemical shift value depends on the degree of alumina condensation.

to correctly differentiate all the contributions of spectra mainly because of peak broadening, it is still possible to identify some species on the catalysts. Pure alumina MPD(0, 0) (Figure 1a) has a single broad signal at 7 ppm that can be assigned to octahedral aluminum Al_{octa} sites.[15] Signal broadening might be partly attributed to the presence of different chemical compounds of aluminum such as $Al(OH_2)_p(OC_2H_4CH(OH)CH_3)_m(OCH(CH_3)C_2H_5)_n$ (where $p + n + m = 6$).[15] The organic ligands come from the alkoxide precursor and from the alcohol solvents used in the synthesis. In catalysts containing Mo [MPD(20, 11) and MPD(30, 0)], P [MPD(0, 11)H], or both elements [MPD(20, 11)H and MPD(30, 11)H], a tail in the spectra between 0 and about −30 ppm is observed (parts b−f of Figure 1). For the last sample, a distinct shoulder at about −5 ppm is also detected. The tail contribution in the spectra seems to increase with increasing amounts of P and Mo. The tail could be due to the presence of new Al octahedral sites, noted Al_{octa}−O−Mo and Al_{octa}−O−P, where molybdenum or phosphorus is located in the second coordination shell of aluminum,[23] or to strongly distorted Al_{octa} sites, which could exhibit large second-order quadrupolar interactions. MPC(20, 0) (Figure 1c) and MPC(30, 0) (Figure 1d) also show a weak signal at ∼60 ppm, which can be assigned to Al_{tetra}.[15] In addition, phosphorus-containing catalysts show a new signal at ∼40 ppm that can be assigned to Al in $AlPO_4$ or more generally to tetrahedral Al sites where phosphorus is located in the second coordination shell of aluminum, noted Al_{tetra}−O−P.[8] The extent of global interaction between P and Al tends to increase in the presence of Mo, since the intensity of the signal at ∼40 ppm is stronger in the Mo-containing MPD(20, 11)H and MPD(30, 11)H catalysts (parts e and f of Figure 1) than that in the Mo-free MPD(0, 11)H catalyst (Figure 1b).

Figure 2 shows the ^{27}Al MAS NMR spectra of the sol−gel catalysts obtained from H_3PO_4 as a P precursor after calcination at 500 °C. Clearly, important modifications are detected by comparison to the dried samples (Figure 1). The MPC(0, 0) catalyst (Figure 2a) has Al_{octa} (the main peak) and tetrahedral aluminum Al_{tetra} sites at ∼65 ppm.[15] Furthermore, a weak and broad component at about 30 ppm is also observed between the two main peaks. This third signal is more clearly detected in the Mo−alumina catalysts such as MPC(20, 0) or MPC(30, 0) (parts c and d of Figure 2). It might be assigned to pentacoordinated aluminum Al_{penta} sites.[16] However, the possibility of building surface tetrahedral Al_{tetra}−O−Mo sites cannot be excluded, since the intensity of this peak increases with increasing amounts of molybdenum. The MPC(0, 11)H sample (Figure 2b) exhibits three distinct signals at 66, 39, and 6 ppm assigned to Al_{tetra}, Al in $AlPO_4$ (Al_{tetra}−O−P), and Al_{octa} sites,

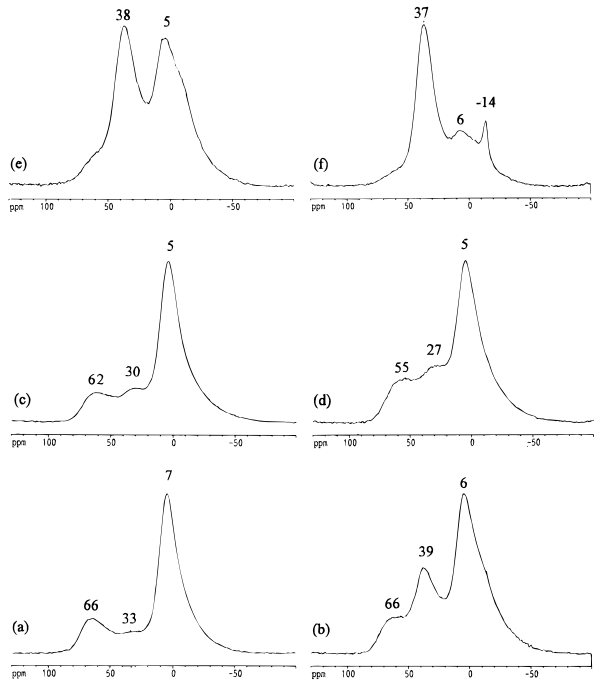

Figure 2. ^{27}Al MAS NMR spectra of Mo−P−alumina based sol−gel catalysts obtained after calcination in air at 500 °C: (a) MPC(0, 0); (b) MPC(0, 11)H; (c) MPC(20, 0); (d) MPC(30, 0); (e) MPC(20, 11)H; (f) MPC(30, 11)H. The P-containing catalysts were prepared with H_3PO_4 as a P precursor.

respectively. Though $AlPO_4$ is already present in the dried state, the intensity of the peak corresponding to the Al_{tetra}−O−P sites clearly increases with calcination. This means that the formation of $AlPO_4$ mainly occurs during calcination, which strengthens the Al−P interactions through the formation of Al−O−P bridges. The calcined Mo−P−alumina catalysts such as MPC(20, 11)H and MPC(30, 11)H (parts e and f of Figure 2) also have Al_{tetra}, Al_{octa} sites, and Al in $AlPO_4$ (Al_{tetra}−O−P) whose NMR characteristics are ∼60, 6, and 37 ppm, respectively. However, their relative populations are strongly dependent on the sample composition. Especially, the catalyst MPC(30, 11)H gives the highest relative amount of $AlPO_4$. It is considered that high loadings of Mo and P facilitate the destruction of γ-alumina and the formation of Al−O−P bridges or of the $AlPO_4$ phase on the catalysts as evidenced by XRD measurements.[2] Moreover, a sharp peak at −14 ppm is also obtained in MPC(30, 11)H (Figure 2f); it corresponds to the presence of $Al_2(MoO_4)_3$.[11] This compound is supposed to be derived from the reaction between bulk MoO_3 and the alumina surface because it is always observed when bulk MoO_3 is present on the alumina.[2,24,25] Schematically, one can write

$$3MoO_3(\text{bulk}) + Al_2O_3(\text{surface}) \rightarrow Al_2(MoO_4)_3$$

However, a weak shoulder around −14 ppm or a tail with negative chemical shifts is essentially observed in all the Mo- and/or P-containing calcined samples as in the case of the dried catalysts. This has been also attributed to the effect of Mo or P in the second coordinative shell of the Al sites or to strongly distorted Al_{octa} sites, which could exhibit large second-order quadrupolar interactions.

Concerning the resonance evolution, the top peak positions of Al_{octa}, Al_{penta}, and Al_{tetra} tend to decrease (in ppm) with increasing the Mo loading. This might be caused by an increase of the alumina framework distortions, which increase the quadrupolar interactions and hence induces the shifts. It also

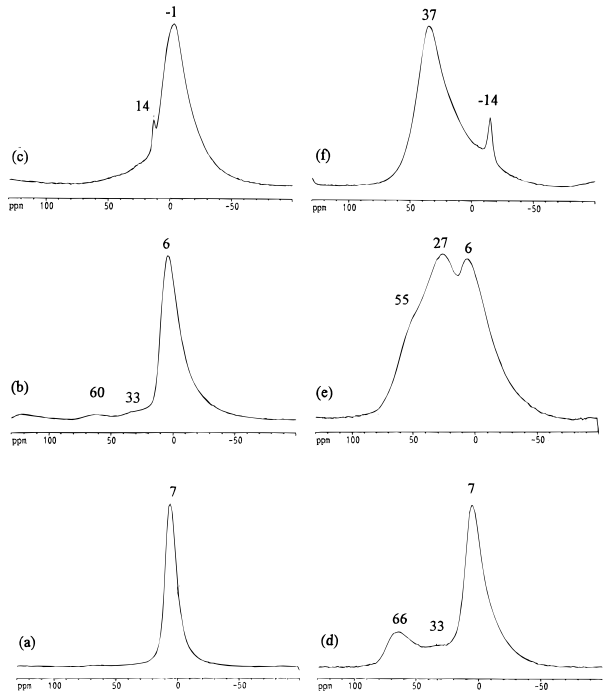

Figure 3. ^{27}Al MAS NMR spectra of dried and calcined Mo−P−alumina based sol−gel catalysts prepared with P_2O_5 as a P precursor. Catalysts obtained after the drying stage at 100 °C were (a) MPD(0, 0), (b) MPD(0, 12)P, and (c) MPD(30, 13)P. Catalysts obtained after calcination at 500 °C were (d) MPC(0, 0), (e) MPC(0, 12)P, and (f) MPC(30, 13)P.

can be due to a decrease of the degree of Al condensation in the gel caused by the presence of Mo.[15,26]

Although ^{27}Al MAS NMR gives useful information on the state of Al in Mo−P−alumina based hydrotreating catalysts, it remains difficult to completely describe the Al sites. These results will be examined again with those obtained by 2D ^{27}Al MQMAS NMR.

(b) Samples Obtained with P_2O_5 as a P Precursor. Figure 3 shows the ^{27}Al MAS NMR spectra of sol−gel catalysts (dried and calcined) obtained with P_2O_5 as a P precursor. For comparison purposes, the spectra of pure alumina [MPD(0, 0) and MPC(0, 0)] are also reported (parts a and d of Figure 3). These spectra are quite different from those obtained with H_3PO_4 as a P precursor. For the dried MPD(0, 12)P catalyst (Figure 3b), two weak features at 60 and 33 ppm with an intense peak at 6 ppm are observed. They correspond to Al_{tetra}, Al_{penta}, and Al_{octa} sites, respectively. For sample MPD(30, 13)P (Figure 3c), an intense and broad signal at −1 ppm is present with a less intense sharp peak at 14 ppm. As already mentioned, the former signal can be assigned to Al_{octa} sites in the gel with a lower degree of condensation.[15] This result suggests that the presence of P_2O_5 in the sample preparation has a detrimental effect on the hydrolysis and condensation steps of the Al *sec*-butylate. Zaharescu et al.[27] also reported that the degree of hydrolysis and condensation of alkoxide is strongly influenced by PO(OR)x complexes in the system of phosphorus−TEOS (tetraethoxysilane $Si(OEt)_4$). The second peak at 14 ppm might be assigned to unreacted alkoxide, to $[Al(OH)_n(H_2O)_{6-n}]_n(MoO_4)$ (with $n = 1$ or 2) or to Al_{penta}−O−P.[10,26,28]

The calcined MPC(0, 12)P sample (Figure 3e) shows three strong signals at 55, 27, and 6 ppm. They can be assigned to Al_{tetra}, Al_{penta}, and Al_{octa} sites as for the dried MPD(0, 12)P catalyst. However, their proportion is considerably different. Especially, the peak intensity of the Al_{penta} site is extremely strong for the calcined sample. This suggests that the structure of MPC(0, 12)P is highly distorted. It is also remarkable that a signal attributed to $AlPO_4$, which should be observed at ∼40 ppm, cannot be detected in sample MPC(0, 12)P, in contrast to the previous MPC(0, 11)H sample (Figure 2b) prepared from H_3PO_4 as a P precursor. This means that the formation of $AlPO_4$ is considerably prevented in the P−alumina catalysts prepared from P_2O_5 as a P precursor in the absence of Mo. However, the Mo−P containing catalyst MPC(30, 13)P (Figure 3f) gives an intense and broad signal at 37 ppm and a smaller sharp signal at −14 ppm, which are assigned to $AlPO_4$ and $Al_2(MoO_4)_3$, respectively. It is inferred again that the presence of Mo leads to the predominant formation of $AlPO_4$ in the series of catalysts prepared from P_2O_5 as a P precursor, as in the case of the previous series prepared from H_3PO_4.

^{31}P MAS NMR. *(a) Samples Obtained with H_3PO_4 as a P Precursor*. Figure 4 shows the ^{31}P NMR spectra of the dried and calcined sol−gel catalysts obtained with H_3PO_4 as a P precursor. In the dried MPD(0, 11)H catalyst (Figure 4a), considering the asymmetric line shape, the broad signal can be decomposed into two overlapping peaks at about −8 and about −21 ppm, which are assigned to monomeric phosphate and polymeric phosphorus oxospecies, respectively.[8] However, Mo−P−alumina catalysts such as MPD(20, 11)H, MPD(30, 5)H, and MPD(30, 11)H (parts b−d of Figure 4) show another characteristic peak at about −15 ppm. This signal could be assigned to a less polymerized P oxospecies. The presence of molybdenum might be effective for dispersing phosphorus oxospecies on the alumina support.

All the calcined catalysts show broad signals (parts e−h of Figure 4) that can be decomposed into peaks at about −18 and about −25 ppm and assigned to polyphosphate and $AlPO_4$, respectively.[7,8] The Mo-containing catalysts such as MPC(30, 5)H and MPC(30, 11)H (parts g and h of Figure 4) show less polyphosphate and then relatively more $AlPO_4$ than the Mo-free MPC(0, 11)H sample (Figure 4e).

(b) Samples Obtained with P_2O_5 as a P Precursor. Figure 5 shows the ^{31}P NMR spectra of selected sol−gel catalysts (dried and calcined) obtained with P_2O_5 as a P precursor. For comparison purposes, the spectra of P−alumina catalysts obtained with H_3PO_4 as a P precursor are also reported. MPD-(0, 12)P (Figure 5b) gives a broad spectrum with an apparent maximum at about −8 ppm, which is mainly assigned to monomeric phosphate species while MPD(0, 11)H (Figure 5a) mainly shows the spectra for polymeric phosphate at −21 ppm.

After calcination, the MPC(0, 12)P catalyst shows an important contribution of polymeric P oxospecies identified by a peak at about −19 ppm (Figure 5e). However, the signal for $AlPO_4$ at about −24 ppm, which is the predominant species in the MPC(0, 11)H sample obtained from H_3PO_4 precursor (Figure 5d), is hardly detected. This is in agreement with the results of ^{27}Al MAS NMR, which did not reveal the presence of such a phase.

To investigate the influence of the nature of the P precursor, liquid ^{31}P NMR spectra of solutions of H_3PO_4 or P_2O_5 in 2-butanol are reported in Figure 6. In the H_3PO_4−butanol solution, only the PO_4^{3-} ions are detected at ∼1 ppm, which indicates a weak solvent effect on the phosphate ions. On the other hand, in the P_2O_5−butanol solution, a lot of sharp peaks around −15 and −27 ppm, which might be attributed to different P alcoholate compounds such as $PO(OH)(OBut)_2$ or $PO(OBut)(OH)_2$, were observed. The small peak at ∼1 ppm arises from traces of water in the solvent, which forms the phosphate ions with P_2O_5. It is suggested that the H_3PO_4 precursor as phosphate

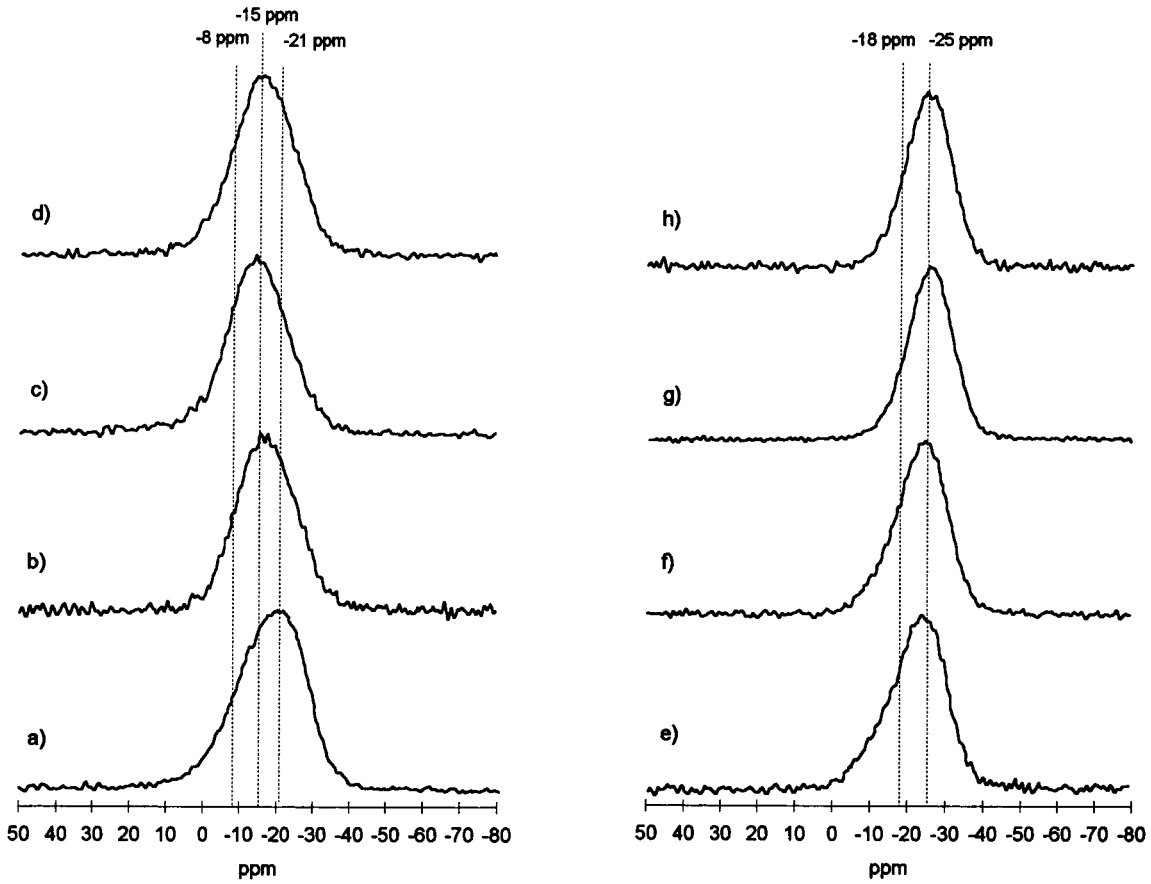

Figure 4. ^{31}P MAS NMR spectra of dried and calcined Mo−P−alumina based sol−gel catalysts prepared with H_3PO_4 as a P precursor. Catalysts obtained after the drying stage at 100 °C were (a) MPD(0, 11)H, (b) MPD(20, 11)H, (c) MPD(30, 5)H, and (d) MPD(30, 11)H. Catalysts obtained after calcination at 500 °C were (e) MPC(0, 11)H, (f) MPC(20, 11)H, (g) MPC(30, 5)H, and (h) MPC(30, 11)H.

ions can easily interact with the alumina framework during its formation and leads to formation of the $AlPO_4$ species, but steric hindrance around phosphorus in P alcoholates should inhibit their interaction during hydrolysis of aluminum *sec*-butylate in the alumina synthesis with P_2O_5 as a precursor.

The dried Mo- and P-containing MPD(30, 13)P catalyst (Figure 5c) gives another signal at −15 ppm, which has been also observed in MPD(30, 11)H (Figure 4d). Since the spectrum at −15 ppm is always detected in the presence of Mo, this signal might also be assigned to Mo−P heteropolycompounds. The calcined MPC(30, 13)P catalyst shows mainly a signal at about −25 ppm (Figure 5f), which is attributed to the $AlPO_4$ species. It is inferred again that the presence of Mo leads to the predominant formation of $AlPO_4$ in the series of catalysts prepared from P_2O_5 as a P precursor, as in the case of the previous series prepared from H_3PO_4.

From the conventional ^{31}P and ^{27}Al MAS NMR spectra, it can be concluded that the affinity of phosphorus with the alumina framework to form $AlPO_4$ depends strongly on the nature of the phosphorus precursor used to prepare the catalysts and also on the presence of Mo.

2D ^{27}Al MQMAS NMR. Figure 7 presents the 2D ^{27}Al MQMAS NMR maps of selected sol−gel catalysts prepared with H_3PO_4 as a P precursor, either after the drying stage or after calcination. Projection of the 3Q-MAS on the horizontal axis (ν_2) gives the 3Q-filtered MAS spectra, which are similar to conventional spectra except that their intensities are modified by quadrupolar MQ excitation. Projection on the vertical axis corresponds to high-resolution spectra that are relieved of quadrupolar broadening. The scales of these sheared spectra have been described in ref 21. The values of the chemical shifts as determined from the resonance gravity centers and therefore corrected for the quadrupolar-induced shift are also listed in Table 2.

The dried alumina sample MPD(0, 0) (Figure 7a) shows a single state at ∼11 ppm corresponding to Al_{octa} sites. This result is in excellent agreement with the ^{27}Al MAS NMR investigation. In the P-containing catalysts such as MPD(0, 11)H (Figure 7c) and MPD(30, 11)H (Figure 7d), a new aluminum site toward lower frequencies can be easily identified at about −5 ppm. This clearly indicates that the tail of ^{27}Al MAS NMR spectra between 0 and about −30 ppm observed in the dried MPD(0, 11)H and MPD(30, 11)H (parts b and f of Figure 1) is attributed to an Al environment such as Al_{octa}−O−P. In addition, a small amount of Al_{tetra}−O−P sites is also observed at ∼45 ppm in these catalysts. On the other hand, the dried Mo−alumina MPD(30, 0) catalyst (Figure 7b) possesses only one type of Al_{octa} site as in the MPD(0, 0) sample and no spectra attributed to Al_{octa}−O−Mo is observed. However, the distortion of the Al_{octa} sites seems to be much more pronounced than the ones present in pure alumina as MPD(0, 0).

After calcination, the pure alumina sample MPC(0, 0) (Figure 7e) presents mainly Al_{octa} and Al_{tetra} sites (10 and 77 ppm, respectively) with a very small amount of Al_{penta} sites at 38 ppm. This also quite agrees with the result of ^{27}Al MAS NMR. The Mo-containing MPC(30, 0) catalyst (Figure 7f) has three components at ∼73, 40, and 11 ppm and assigned to Al_{tetra}, Al_{penta}, and Al_{octa} sites, respectively. The presence of Mo introduces a large distortion into the alumina framework, since a significant intensity increase of the Al_{penta} feature is observed by comparison with the MPC(0, 0) catalyst. The 2D map of the MPC(0, 11)H sample (Figure 7g) is similar to the one of

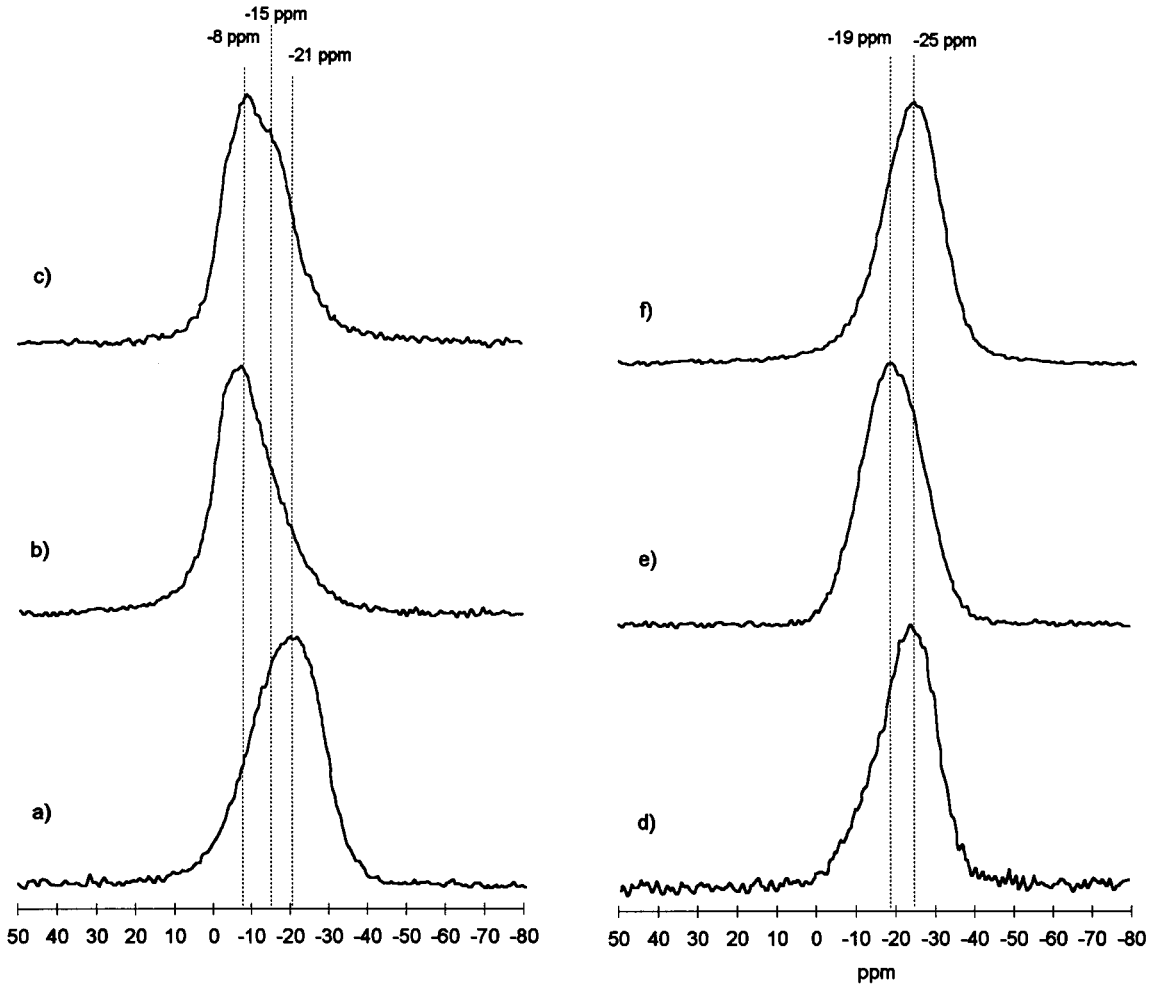

Figure 5. Comparison of ^{31}P MAS NMR spectra of dried and calcined Mo−P−alumina based sol−gel catalysts prepared from P_2O_5 and H_3PO_4 as P precursors. Catalysts obtained after the drying stage at 100 °C were (a) MPD(0, 11)H, (b) MPD(0, 12)P, and (c) MPD(30, 13)P. Catalysts obtained after calcination at 500 °C were (d) MPC(0, 11)H, (e) MPC(0, 12)P, and (f) MPC(30, 13)P.

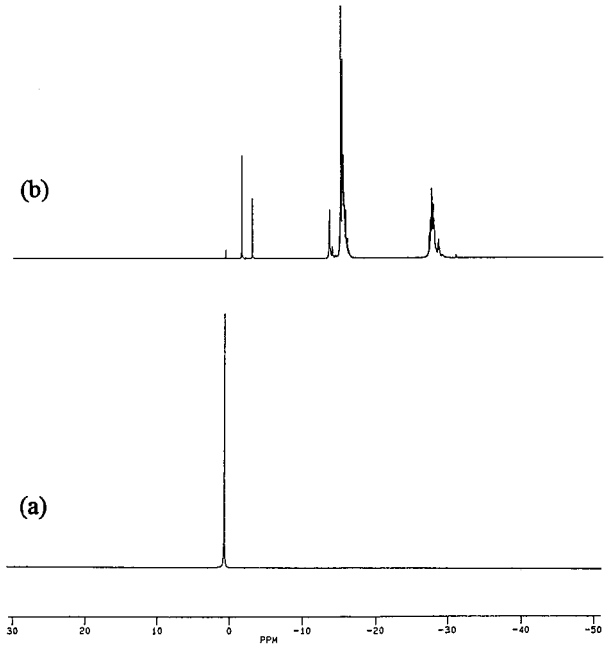

Figure 6. Liquid ^{31}P NMR spectra of the solutions with the P precursors used to prepare the sol−gel catalysts: (a) H_3PO_4 dissolved in 2-butanol; (b) P_2O_5 dissolved in 2-butanol.

the MPC(30, 0) catalyst (Figure 7f). The maximum of the two peaks at 77 and 12 ppm can be assigned to Al_{tetra} and Al_{octa} sites, respectively, as in the case of MPC(30, 0). However, considering the results of ^{27}Al MAS NMR and the spectra projection around 40 ppm to the left showing small doublets, the MPC(0, 11)H sample (and also the MPC(30, 11)H sample) must contain two different species around ∼40 ppm that can be decomposed into Al_{penta} and Al_{tetra}−O−P sites, respectively. In addition, it is noted that P-containing calcined catalysts MPC-(0, 11)H and MPC(30, 11)H (parts g and h of Figure 7) do not show a spectrum around −5 ppm, since it was clearly observed in the corresponding dried catalysts. Therefore, the shoulder or tail around −14 ppm observed in the ^{27}Al MAS NMR measurement of calcined catalysts (Figure 2) can be considered as highly distorted Al_{octa} sites while those in the dried catalysts are attributed to the Al_{octa}−O−P sites. In the MPC(30, 11)H catalyst (Figure 7h), a strong peak at 42 ppm is mainly observed. Contribution of the other Al_{octa}, Al_{penta}, and Al_{tetra} sites is very weak. This confirms that large loadings of Mo and P tend to destroy the structure of γ-alumina and facilitate the formation of the $AlPO_4$ phase. The spectrum of $Al_2(MoO_4)_3$ around −15 ppm is not observed by 2D MQMAS NMR in the MPC(30, 11)H sample. It might be difficult to detect such a sharp and rather weak peak under these experimental conditions.

Considering the 2D maps presented in Figure 7, it is obvious that 2D ^{27}Al MQMAS NMR gives interesting information on the state of Al in highly divided alumina-based catalysts owing to its high resolution and the results complete those obtained by conventional ^{27}Al MAS NMR.

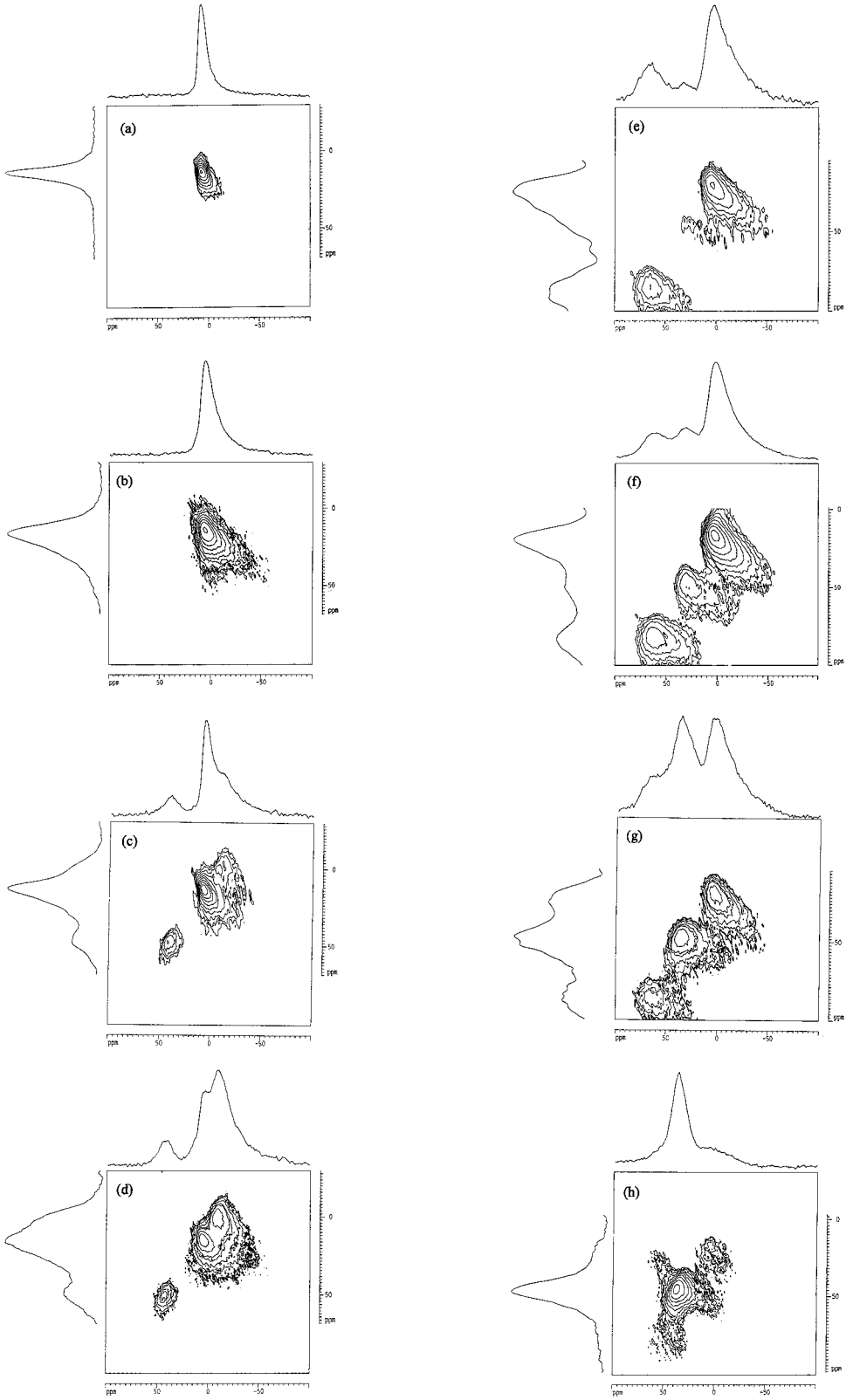

Figure 7. Shared 2D ^{27}Al MQMAS NMR spectra of Mo−P−alumina based sol−gel catalysts. The P-containing catalysts were prepared with H_3PO_4 as a P precursor. Catalysts obtained after the drying stage at 100 °C were (a) MPD(0, 0), (b) MPD(30, 0), (c) MPD(0, 11)H, and (d) MPD(30, 11)H. Catalysts obtained after calcination at 500 °C were (e) MPC(0, 0), (f) MPC(30, 0), (g) MPC(0, 11)H, and (h) MPC(30, 11)H.

Conclusion

Molybdenum oxide−phosphorus oxide−alumina sol−gel catalysts with a wide range of P loading (from 0 to 11 wt % of P) were prepared to elucidate the effect of phosphorus on the states of Al and P. The amount of phosphorus and the nature of the P precursors (H_3PO_4 or P_2O_5) affect them significantly. Aluminum mainly exists in octahedral, tetrahedral, and penta-coordinated environments. P-containing catalysts also possess mainly Al_{octa}−O−P sites after the drying stage and Al_{tetra}−O−P sites after calcination. The use of P_2O_5 seems to strongly

TABLE 2: Chemical Shifts Obtained by 2D ^{27}Al MQMAS NMR on Selected Mo−P−Alumina Based Sol−Gel Catalysts

catalysts	chemical shift (ppm)	catalysts	chemical shift (ppm)
MPD(0, 0)	11	MPC(0, 0)	77, 38, 10
MPD(0, 11)H	45, 11, −5	MPC(0, 11)H	77, (42),[a] (39),[a] 12
MPD(30, 0)	11	MPC(30, 0)	73, 40, 11
MPD(30, 11)H	47, 11, −5	MPC(30, 11)H	42, 12

[a] The peaks are not clearly identified.

prevent hydrolysis and condensation of the aluminum *sec*-butylate. In dried catalysts, P is supported as monomeric or polymeric P oxospecies when using H_3PO_4, while P is supported as organic monomeric P oxospecies when using P_2O_5. In calcined samples, the H_3PO_4 precursor favors the formation of the $AlPO_4$ phase (Al_{tetra}−O−P surface species) while the P_2O_5 precursor leads to form polymeric P oxospecies in the absence of Mo. In any case, the presence of Mo favors the interaction of phosphorus with the alumina support and leads to the formation of $AlPO_4$.

It is concluded that the combination of conventional ^{27}Al and ^{31}P MAS NMR with 2D ^{27}Al MQMAS NMR is extremely useful for elucidating the precise states of Al and P species in Mo−P−Al based hydrotreating catalysts.

Acknowledgment. The authors thank Dr. Revel and Dr. Watkin (from the "Centre Commun de Mesures RMN" of Université des Sciences et Technologies de Lille (USTL), Villeneuve d'Ascq, France) and Professor Guelton and Dr. Rigole (Laboratoire de Catalyse Hétérogène et Homogène, USTL) for their continuous help and/or technical support. The authors also thank Dr. Kraus (Laboratory for Technical Chemistry, Swiss Federal Institute of Technology, Switzerland) for giving us useful information on the MAS NMR investigation. The "Région Nord-Pas de Calais" is acknowledged for financial support for the purchase of the ASX400 and ASX100 spectrometers. One of the authors (R.I.) also thanks the Japan Cooperation Center Petroleum (JCCP) for a financial support.

References and Notes

(1) Le Bihan, L.; Mauchaussé, C.; Duhamel, L.; Grimblot, J.; Payen, E. *J. Sol−Gel Sci. Technol.* **1994**, *2*, 837.
(2) Iwamoto, R.; Grimblot, J. *Stud. Surf. Sci. Catal.* **1997**, *106*, 195.
(3) Eijsbouts, S.; Van Gestel, J.; van Veen, J. A. R.; de Beer, V. H. J.; Prins, R. *J. Catal.* **1991**, *131*, 412.
(4) Lewis, J. M.; Kydd, R. A. *J. Catal.* **1992**, *136*, 478.
(5) Jian, M.; Prins, R. *Catal. Lett.* **1995**, *35*, 193.
(6) Poulet, O.; Hubaut, R.; Kasztelan, S.; Grimblot, J. *Bull. Soc. Chim. Belg.* **1991**, *100*, 857.
(7) Han, O. H.; Lin, C. Y.; Haller, G. L. *Catal. Lett.* **1992**, *14*, 1.
(8) De Canio, E. C.; Edwards, J. C.; Scalzo, T. R.; Storm, D. A.; Bruno, J. W. *J. Catal.* **1991**, *132*, 498.
(9) Cheng, W. C.; Luthra, N. P. *J. Catal.* **1988**, *109*, 163.
(10) Edwards, J. C.; De Canio, E. C. *Catal. Lett.* **1993**, *19*, 121.
(11) Cho, H.; Park, S. B.; Kwak, J. H. *J. Mol. Catal.* **1996**, *A104*, 285.
(12) Kraus, H.; Prins, R. *J. Catal.* **1996**, *164*, 251.
(13) Kraus, H. Ph.D. Thesis, ETH Zürich, Switzerland 11620, 1996.
(14) Kraus, H.; Prins, R. *J. Catal.* **1997**, *170*, 20.
(15) Kurokawa, Y.; Kobayashi, Y.; Nakata, S. *Heterog. Chem. Rev.* **1994**, *1*, 309.
(16) Risbud, S. H.; Kirkpatrick, R. J.; Taglialavore, A. P.; Montez, B. *J. Am. Ceram. Soc.* **1987**, *70* (1), C10.
(17) van Eck, E. R. H.; Kentgens, A. P. M.; Kraus, H.; Prins, R. *J. Phys. Chem.* **1995**, *99*, 16080.
(18) Kraus, H.; Prins, R.; Kentgens, A. P. H. *J. Phys. Chem.* **1996**, *100*, 16336.
(19) Fernandez, C.; Amoureux, J. P.; Chezeau, J. M.; Delmotte, L.; Kesseler, H. *Microporous Mater.* **1996**, *6*, 331.
(20) Fernandez, C.; Amoureux, J. P. *Chem. Phys. Lett.* **1995**, *242*, 449.
(21) Amoureux, J. P.; Fernandez, C. *Solid State Nucl. Magn. Reson.*, in press.
(22) Amoureux, J. P.; Fernandez, C.; Steuernagel, S. *J. Magn. Reson.* **1996**, *A123*, 116.
(23) Bautista, F. M.; Campelo, J. M.; Garcia, A.; Luna, D.; Marina, J. M.; Romero, A. A. *Appl. Catal.* **1993**, *96*, 175.
(24) Ramirez, J.; Castano, V. M.; Leclercq, C.; López Agudo, A. *Appl. Catal. A* **1992**, *83*, 251.
(25) López Cordero, R.; López Guerra, S.; Fierro, J. L. G.; López Agudo, A. *J. Catal.* **1990**, *126*, 8.
(26) Rezgui, S.; Gates, B. C. *Chem. Mater.* **1994**, *6*, 2386.
(27) Zaharescu, M.; Vasilescu, A.; Badescu, V.; Radu, M. *J. Sol−Gel Sci. Technol.* **1997**, *8*, 59.
(28) Brow, R. K.; Kirkpatrick, R. J.; Turner, G. L. *J. Am. Ceram. Soc.* **1990**, *73* (8), 2293.